The δapproximation (reflection) method applied to a twophoton process

P. Baierl and W. Kiefer

Citation: The Journal of Chemical Physics **77**, 1693 (1982); doi: 10.1063/1.444066
View online: http://dx.doi.org/10.1063/1.444066
View Table of Contents: http://scitation.aip.org/content/aip/journal/jcp/77/4?ver=pdfcov
Published by the AIP Publishing

The δ-approximation (reflection) method applied to a two-photon process

P. Baierl and W. Kiefer

Physikalisches Institut der Universität Bayreuth, Postfach 3008, D-8580 Bayreuth, Federal Republic of Germany

(Received 1 June 1981; accepted 1 September 1981)

The δ-approximation or reflection method, which is able to well explain continuous absorption spectra of diatomics has been applied for a two-photon process. It is shown to what extent this approximation can be employed for the description of the band profiles observed in a Raman scattering process in $^{79}Br_2$, where resonance takes place with the continuum of a repulsive and a dissociative excited electronic state. By means of this approximation, simple diagrams can be drawn which allow a qualitative explanation of the change in band profiles of resonantly enhanced vibrational–rotational Raman transitions.

I. INTRODUCTION

In order to derive the intensity distribution in continuous absorption spectra of diatomic molecules, a simple but highly efficient approximation, the so-called δ-approximation or reflection method has already been introduced by Condon[1] and by Winans and Stueckelberg[2,3] in 1928. In addition, a number of other useful approximations[4–7] have been developed for calculating Franck–Condon factors (FCF's) in many problems involving diatomic molecules. However, the reflection method for bound–continuum transitions seems to be most widely used.[1–3,8–17] This approximation method treats the radial wave function of the continuum state like a δ-function centered at the classical turning point, while retaining the true form of the wave function of the electronic ground state. The overlap integral is therefore simply the value of the discrete wave function at the turning point of the state in the continuum, and the distribution of radiation intensity can be found from the square of this function by projecting it upon the vertical energy axis by means of the repulsive or dissociative potential curve, and multiplying it by the proper frequency factor. In order to simplify the following discussion for a two-photon process (continuum resonance Raman scattering), we first demonstrate the reflection method for a one-photon process (absorption) in a system with two continuum states. The same system will then be used for the two-photon process. In Fig. 1 the ground state potential curve ($^1\Sigma_{g^+}$) as well as the excited state repulsive ($^1\Pi_{1u}$) and bound [$B(^3\Pi_{0^+u})$] potential curves are drawn to scale for $^{79}Br_2$. The construction of the theoretical absorption intensity distribution according to the δ-approximation method is also illustrated graphically in this figure. The normalized eigenfunction of the vibrational ground state ($v'' = 0$), which has the same abscissa scale as the potential functions, but of course a different ordinate scale (not given in the figure), is reflected at the upper two potential curves of state B and $^1\Pi$, onto the energy axis resulting in the two functions ψ'_B and $\psi'_{1\Pi}$, respectively. The vertical and horizontal lines indicate the "reflection." The functions $(\mathfrak{M}_B)^2\psi'^2_B$ and $(\mathfrak{M}_{1\Pi})^2\psi'^2_{1\Pi}$, also shown on the left side of Fig. 1, are obtained by squaring the ψ' functions and multiplying them by the appropriate electric transition moment $\mathfrak{M}$ ($\mathfrak{M}^2_{1\Pi}/\mathfrak{M}^2_B = 2$ was taken for this purpose, a value which is approximately the average value given in Refs. 10 and 18). Thus, if these curves are multiplied by the frequency ν and added algebraically, one obtains, except for a constant factor, the calculated absorption coefficient as a function of frequency. The heavy line drawn to the left in Fig. 1 shows the calculated absorption spectrum obtained in this way for the $^{79}Br_2$ mole-

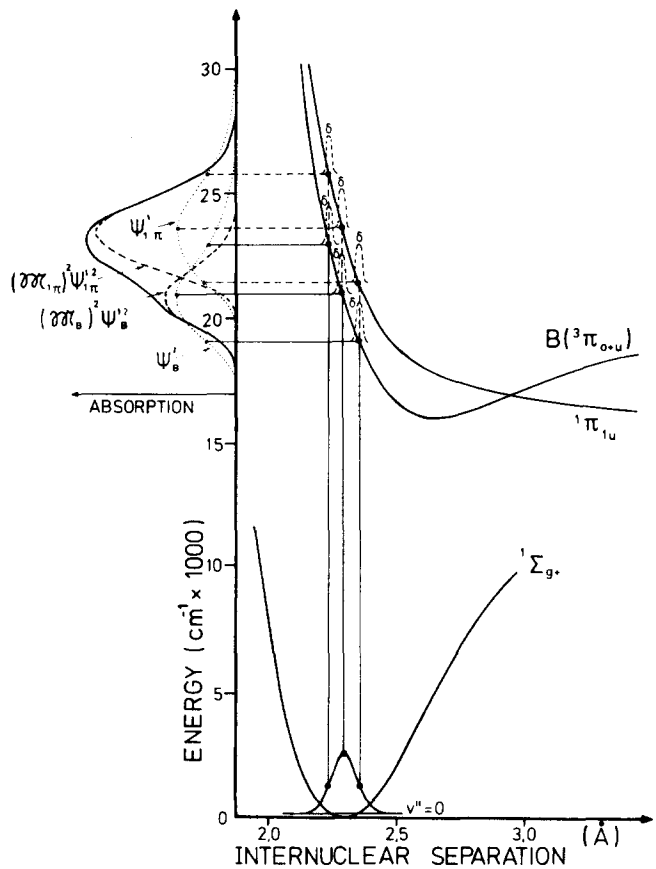

FIG. 1. The reflection method (δ approximation) applied to a one-photon process. The continuous absorption spectrum of diatomic bromine ($^{79}Br_2$) is obtained by reflecting the wave function ψ of the vibrational ground state ($v'' = 0$) by the two excited electronic states B and $^1\Pi$. The functions obtained ψ'_B and $\psi'_{1\Pi}$ are then squared and multiplied by the square of the pure electronic transition moment to result in $(\mathfrak{M}_B)^2\psi'^2_B$ and $\mathfrak{M}_{1\Pi})^2\psi'^2_{1\Pi}$. The algebraic sum of these two terms gives the absorption spectrum (heavy line on the left side). The multiplication by the frequency ν is omitted for simplicity. The dotted curve denoted by δ is to be thought of as infinitely thin and infinitely high, so that the area under it is unity. The vertical and horizontal lines serve to guide the "reflection."

 0021-9606/82/161693-08$02.10

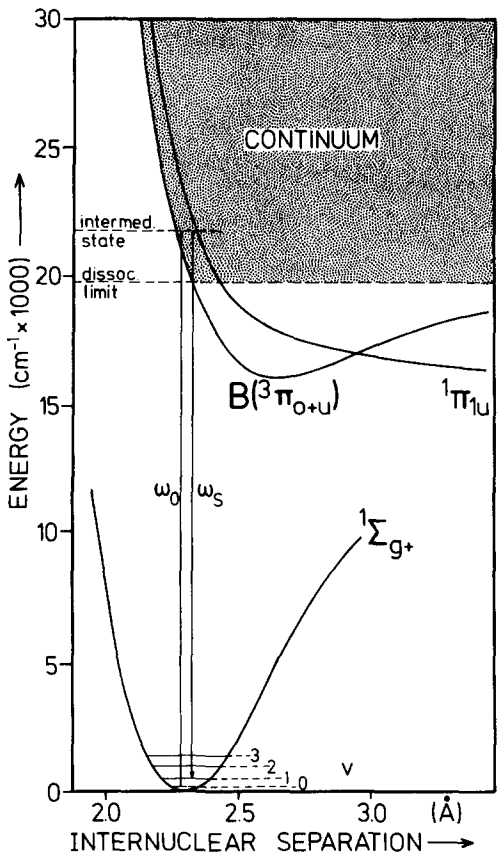

FIG. 2. Schematic diagram for continuum resonance Raman scattering in bromine vapor ($^{79}Br_2$). The vertical lines indicate a two-photon process ($\Delta v = 1$, $1 \leftarrow 0$ vibrational transition), which is in resonance with two electronic continuum states ($^3\Pi_{0+u}$, $^1\Pi_{1u}$). ω_0, ω_s denote frequency of exciting laser beam and of scattered Raman light, respectively.

cule. This spectrum is in fairly good agreement with the experimental one.[10,18]

II. APPLICATION OF THE δ APPROXIMATION TO CONTINUUM RESONANCE RAMAN SCATTERING IN DIATOMICS

The reason for the widespread use of the δ approximation in absorption calculation and analysis certainly is its conceptual and computational simplicity combined with the surprisingly good results when compared to complete calculations. Therefore, the question arises if this method is also able to quantitatively describe two-photon processes in which the products of two FCF's are involved. Such a case is given, for instance, in resonance Raman scattering (RRS) by a continuum in diatomic molecules.[19,20] The scheme for resonance Raman scattering via continuum states is demonstrated in Fig. 2, where we show again (compare Fig. 1) the electronic states for the $^{79}Br_2$ molecule. The two vertical lines elucidate the two-photon process for a $\Delta v = 1$ Raman transition, where a photon with frequency ω_0 is incident and the Stokes-shifted photon with frequency ω_s is scattered. The intermediate state lies above the dissociation limit of bound state B and hence scattering occurs via levels in the two continuum electronic states, i.e., the repulsive state $^1\Pi_{1u}$ and the dissociative state B.

One of the most striking features of RRS is the presence of prominent vibrational progressions. Mingardi and Siebrand[21,22] were able to give a qualitative explanation of the intensity distribution in RR progressions by applying the δ-approximation method described above. A simple model potential function for the excited state was used by these authors in order to obtain an analytical solution. Similar models in connection with the δ approximation were also used by Jacon and van Labeke.[23] However, these theories were only suitable to explain in a general way particular features in RRS. No attempt was made to quantitatively calculate RRS spectra and their frequency dependence for a real scattering system in order to be able to compare the theoretically constructed with experimentally obtained spectra, as has been done for absorption spectra. To our knowledge, the only quantitative study in this respect was performed by Fenstermacher and Callender,[24] who reported measurements of the visible absorption and Raman intensity dispersion of I_2 molecules dissolved in chloroform. While the absorption spectrum was adequately interpreted by means of the δ-function model and by a Morse-type potential function with constants measured in gaseous iodine[25] to represent the excited electronic state, the model gave relatively unsatisfactory fits to the Raman dispersion data. The authors have discussed the relatively poor agreement between calculated Raman dispersion curves with the measured results in terms of various possible sources. Among others, solvent effects on the gas molecular potential curves certainly play an important role here, since the resonant Raman scattering intensity is very sensitive to the curvature and position of the potential curves (see below). A study of this type in the liquid phase without knowledge of the accurate potential functions is therefore inadequate to test the applicability of the δ-approximation method.

In the last decade we have performed extensive experimental and theoretical work on continuum RRS in iodine and in natural as well as isotopically pure bromine gas.[26–37] A comprehensive theory was developed[36] which was applied[37] to make first principle calculations of RR band profiles, which have been also obtained experimentally[27,28,31,32] for I_2 and Br_2 molecules. Very good agreement between experiment and theory was obtained. Therefore, these RRS systems can serve now to check the applicability of the δ approximation to describe quantitatively this type of a two-photon process. This will be discussed in more detail below.

A. Comprehensive theory

In Refs. 36 and 37 we have derived closed expressions which allow a first principle calculation of the continuum resonance Raman intensity of a single vibrational–rotational transition $f \leftarrow i(v' \leftarrow v'', J' \leftarrow J'')$. The basic formulas have been deduced for halogen molecules which have two excited states $B\,(^3\Pi_{0+u})$ and $^1\Pi_{1u}$ contributing to the overall resonance Raman scattering intensity for this particular transition. The final expressions for these calculations are given in Eqs. (1)–(4) of Ref. 37. Scattering experiments in halogen gases with cw lasers[28,32] as excitation sources revealed that high spectroscopic temperatures are involved. Therefore, in

order to do the correct calculation of the total band shape of the same vibrational transitions ($\Delta v = n$, n = integer), one has to sum over all populated vibrational and rotational levels in the electronic ground state. This summation finally results in the total band shape obtained for a particular vibrational transition (e.g., $\Delta v = 1$ fundamental Raman band, see below). Results of these comprehensive theory have already been published by us in Ref. 37 and they will be partially shown again (for ease of comparison) in Figs. 9–13 together with the experimentally[32] obtained spectra and the spectra obtained theoretically applying the δ approximation.

B. δ-approximation method

Inspecting Eqs. (3) and (4) of Ref. 37 one notices that both real and imaginary parts of the Raman scattering amplitude, with contributions from the two electronic states B and $^1\Pi$, contain products of two vibrational overlap factors (VOF) of form: $\langle v' | v_e \rangle \langle v_e | v'' \rangle$. For ease of discussion we term the factor $\langle v_e | v'' \rangle$ as VOF for the "absorption" process, because it describes the vibrational transition from the initial state v'' to the vibrational state v_e of the excited state continuum (intermediate state of the two-photon process). The other factor of the product describes the transition from the intermediate down to the final vibrational state v' of the electronic ground state. We therefore label this as the VOF for the "re-emission" process. In the δ-approximation method the wave functions $|v_e\rangle$ are now simply replaced by δ functions for both VOF's. This has the consequence that the VOF for the "absorption" process is simply the value of the vibrational radial wave function which describes the initial state, taken at the classical turning point of the continuum resonance state. Similarly, one finds the VOF for the re-emission process as correspondent value of the vibrational wave function of the final state.

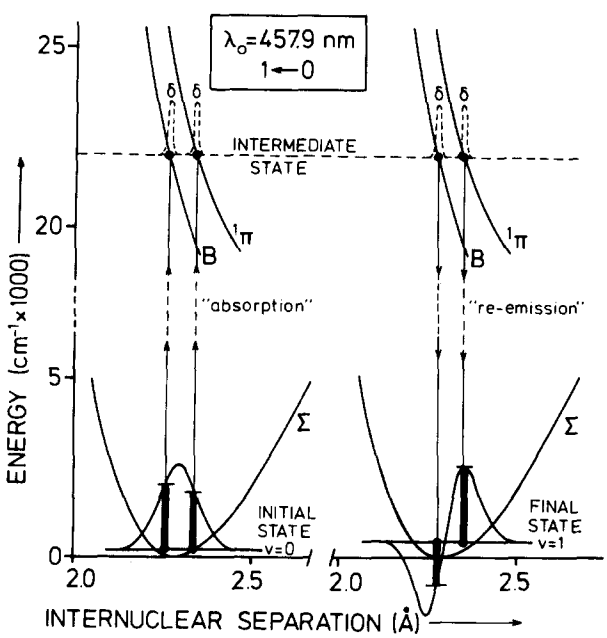

FIG. 3. The δ-approximation method applied to a two-photon process. The continuous resonance Raman scattering amplitude for the fundamental of diatomic bromine ($^{79}Br_2$) is obtained by replacing the upper state wave functions with δ functions located at the classical turning point. The vertical heavy bars (electronic ground state) represent the values of the vibrational overlap factors (VOF's) for the "absorption" process (left field) and for the "re-emission" process (right field) for the two excited states B and $^1\Pi$. Excitation wavelength $\lambda_0 = 457.9$ nm. Vibrational transition: $v' = 1 \leftarrow v'' = 0$.

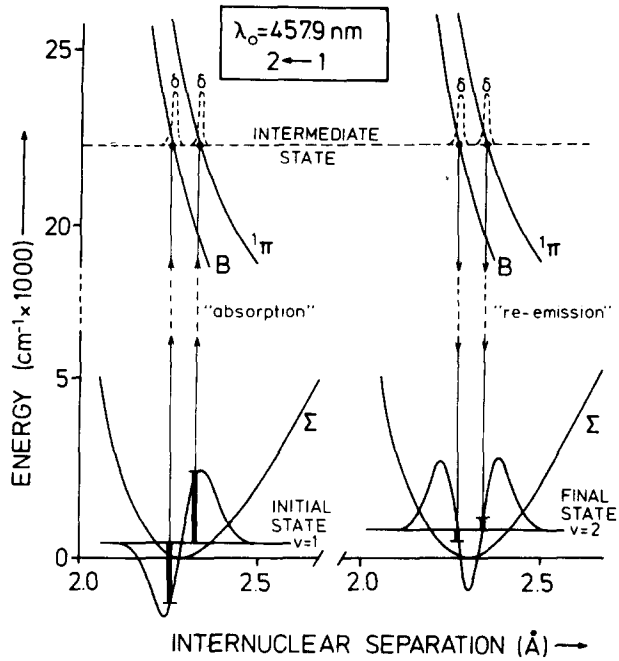

FIG. 4. Captions as in Fig. 3 except for vibrational transition: $v' = 2 \leftarrow v'' = 1$.

In order that closure over the complete set of energy-normalized continuum functions is insured, the δ functions are to be multiplied by the normalization factor $(-dR/dV)^{1/2}$ (see Ref. 38), where R is the internuclear separation and V the associated potential function. The shapes of the potential functions considered in this paper are only slowly varying functions with energy (compare the two potential functions in Fig. 2). Numerical calculations of the slopes $(\partial V/\partial R)_\Pi$ and $(\partial V/\partial R)_B$ for the energy range of interest showed that the normalization factor can indeed be treated as a constant, without making too large an error.

The simple approach of describing qualitatively continuum RR vibrational intensities as discussed above is illustrated in Figs. 3 and 4, where we have drawn the radial wave functions for initial and final vibrational states as well as the potential functions (Σ, B, Π) to scale for $^{79}Br_2$ and for the $\Delta v = 1$ (fundamental) Raman transitions $v' = 1 \leftarrow v'' = 0$ (Fig. 3), $v' = 2 \leftarrow v'' = 1$ (Fig. 4), and $v' = 3 \leftarrow v'' = 2$ (Figs. 5 and 6). Figures 5 and 6 differ only in respect to the excitation wavelength λ_0 employed, which is 457.9 nm for Fig. 5 and 488.0 nm for Fig. 6, respectively. The vertical heavy bars in these figures represent the values of the VOF's for the absorption process (left field) and for the re-emission process (right field). The left bar in each field corresponds to the VOF associated to the dissociative B state while the

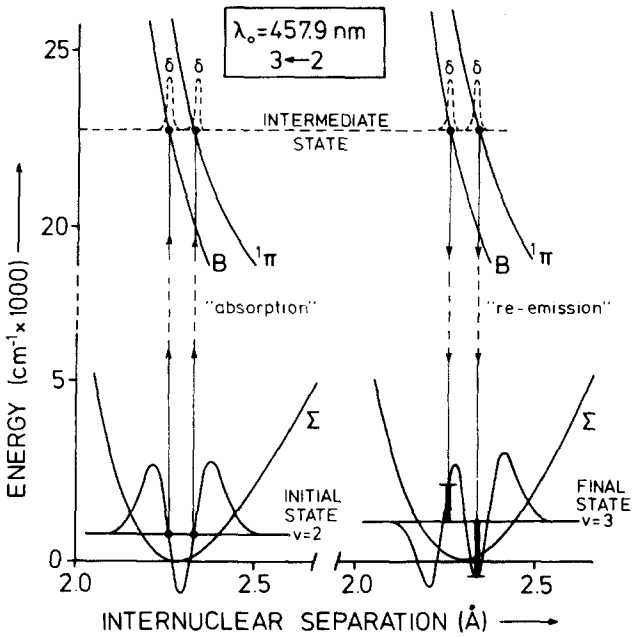

FIG. 5. Captions as in Fig. 3 except for vibrational transition: $v' = 3 \leftarrow v'' = 2$.

right bar in each field is the value for the VOF assigned to the repulsive Π state. It should be mentioned here that the way of representing the Raman scattering process as illustrated in Figs. 3–6 does not mean that there is an appreciable time delay between absorption and re-emission, as is the case for discrete resonance Raman scattering[39] (resonance fluorescence), where the scattering time is in the range of 10^{-5}–10^{-8} s. The virtual separation into an absorption and re-emission process and the double presentation of two excited states in Figs. 3–6 was done only for ease of discussion and for

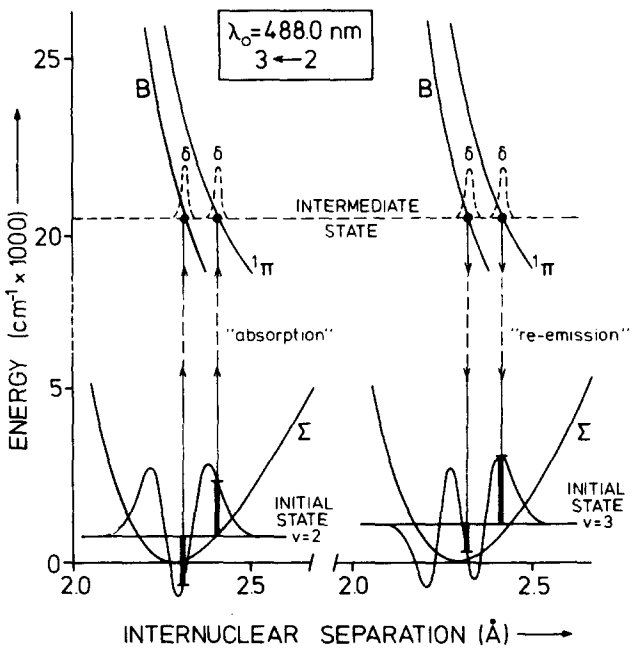

FIG. 6. Captions as in Fig. 3 except for excitation wavelength $\lambda_0 = 488.0$ nm and vibrational transition: $v'' = 3 \leftarrow v'' = 2$.

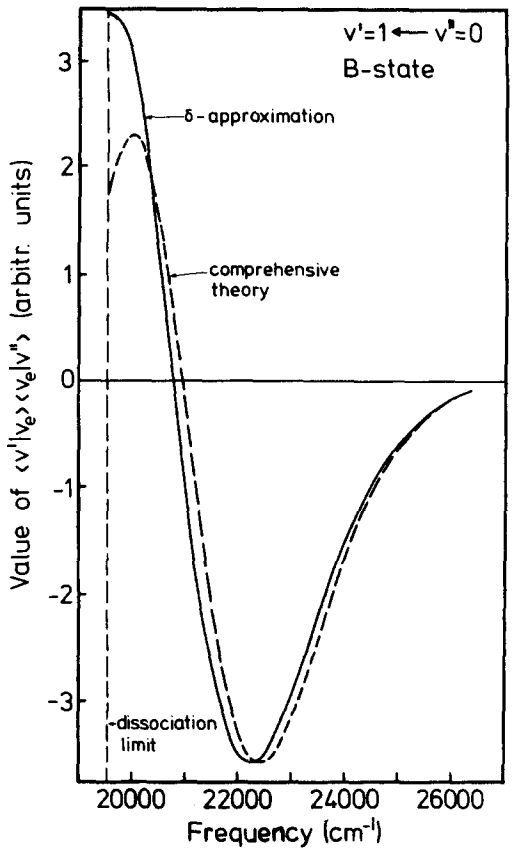

FIG. 7. The value of the product of two matrix elements $(\langle \psi' | v_e \rangle \langle \psi_e | v'' \rangle)$ as a function of frequency, calculated for the $v' = 1 \leftarrow v'' = 0$ Raman transition in $^{79}Br_2$. Calculations were performed for resonance with the continuum of the B state only.

making the presentation more transparent. As will be shown later, these diagrams facilitate very much the qualitative description of the intensity behavior of particular vibrational transitions when the excitation frequency is varied.

III. RESULTS AND DISCUSSION

In order to test the applicability of the reflection method to a two-photon process, we first make an explicit comparison between the comprehensive theory and the δ-approximation method for a specific vibrational transition. We have calculated the product of the transition matrix elements $(\langle v' | v_e \rangle \langle v_e | v'' \rangle)$ for the $v' = 1 \leftarrow v'' = 0$ resonance Raman transition in $^{79}Br_2$ employing the comprehensive theory.[36,37] The value of this product, determined as a function of exciting frequency, is compared to the correspondent value obtained by means of the δ approximation. Results are presented graphically in Figs. 7 and 8. Here, the contributions from the two excited states are displayed separately (Fig. 7: B state; Fig. 8: $^1\Pi$ state). Except for energies close to the dissociation limit (see below), there is fairly good agreement between results obtained with the comprehensive theory and the δ-approximation method when the two curves in Fig. 7 are compared to each other. Similar good agreement was obtained for contributions arising from resonance with the $^1\Pi$ state (Fig. 8).

Comparison of the comprehensive theory as well as of the δ-approximation method with experimental data can only be made when thermally averaged $\Delta v = 1$ spectra are calculated as discussed in Ref. 37. This has been done for the fundamental region of $^{79}Br_2$, where continuum resonance Raman scattering can be performed through excitation with some lines of an argon ion laser. These lines have wavelengths of 457.9, 476.5, 488.0, 496.5, and 501.7 nm. The line at 514.5 nm produces resonance fluorescence.[19] Using the lines with $\lambda_0 \leqq 501.7$ nm, experiments were performed and the experimental spectra relating to the fundamental vibration ($\Delta v = 1$) are shown in the upper fields of Figs. 9–13. Remarkable changes in the band profiles can be seen. In each of these figures, the second spectrum from the top is the one calculated by employing the comprehensive theory,[36,37] whereas the spectra in the lower parts of Figs. 9–13 are the result of calculations where the radial wave functions of the continuum states have been replaced by δ functions. These figures demonstrate the excellent agreement between the experimental spectra and those which have been calculated employing the comprehensive theory for all exciting wavelengths. The spectra calculated by means of the δ approximation also agree fairly well for the excitation wavelengths 457.9 nm (Fig. 9), 476.5 nm (Fig. 10), and 488.0 nm (Fig. 11). Discrepancies occur only for excitation close to the dissociation limit. Note for instance, that the $v' = 2 \leftarrow v'' = 1$ transition comes out too high in intensity for $\lambda_0 = 496.5$ (Fig. 12) and 501.7 nm (Fig. 13) excitation. However, in general the error made by using the δ approximation is not too high for the cases shown in this study.

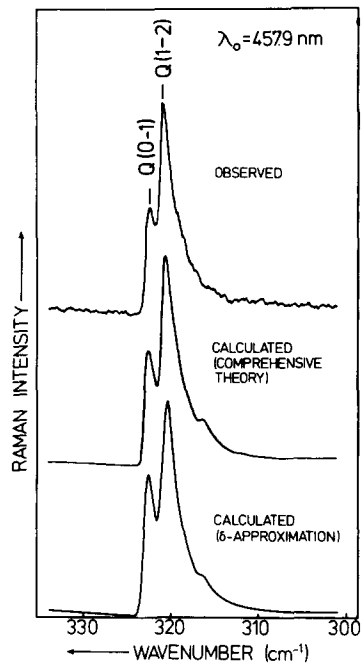

FIG. 9. Experimentally observed[32] (upper spectrum) and calculated (middle and lower spectra) band profiles for the $\Delta v = 1$ Raman transition (fundamental vibration) in $^{79}Br_2$ for $\lambda_0 = 457.9$ nm excitation. Calculations were performed using the comprehensive theory[36,37] (middle spectrum) as well as the δ-approximation method (lower spectrum).

As known, the δ approximation applied to a one-photon process works well for steep upper repulsive potentials because the error made in replacing the upper state wave functions with the δ function goes approximately as the inverse cube of the slope at the classical turning point.[40] Our results also demonstrate this at least quali-

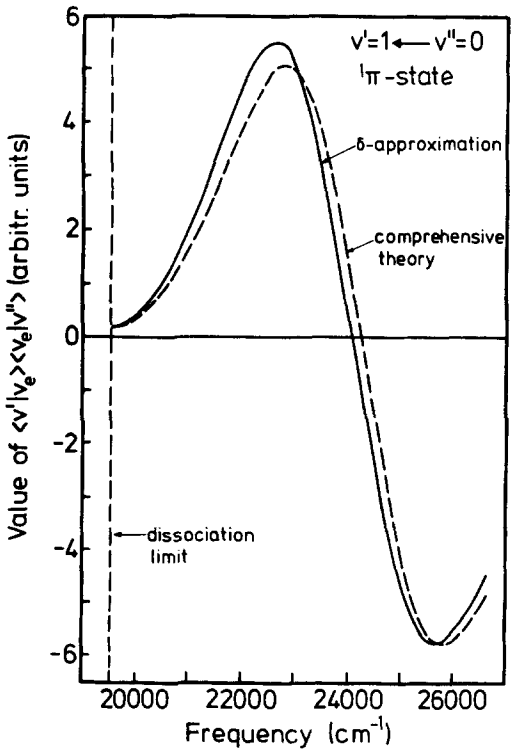

FIG. 8. Captions as in Fig. 7 except for the resonance state, which is here the $^1\Pi$ state.

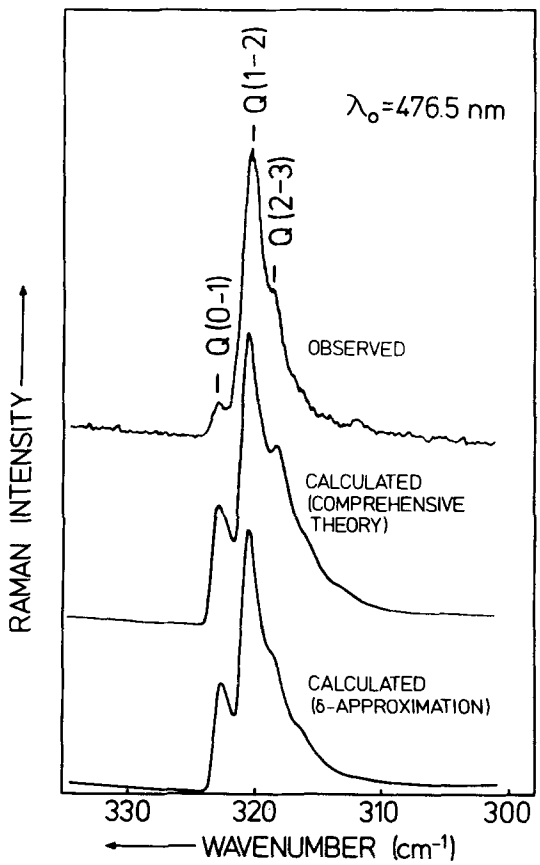

FIG. 10. Captions as in Fig. 9 except for excitation wavelength $\lambda_0 = 476.5$ nm.

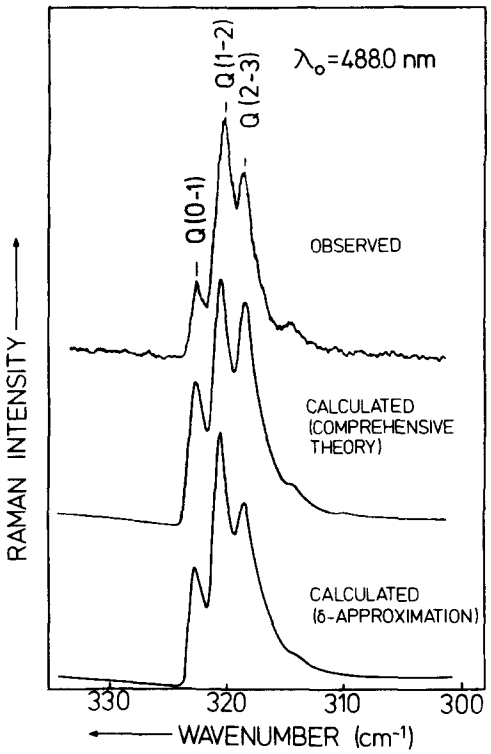

FIG. 11. Captions as in Fig. 9 except for $\lambda_0 = 488.0$ nm.

tatively. As mentioned already above, discrepancy occurs mainly for the $2 \leftarrow 1$ vibrational transition for low energetic excitation. We found[37] that for the excitation wavelengths 496.5 and 501.7 nm, the $1 \leftarrow 0$ transition gets its intensity mainly from the B state, whereas the transitions $2 \leftarrow 1$ and $3 \leftarrow 2$ are generated through resonance with the $^1\Pi$ state.

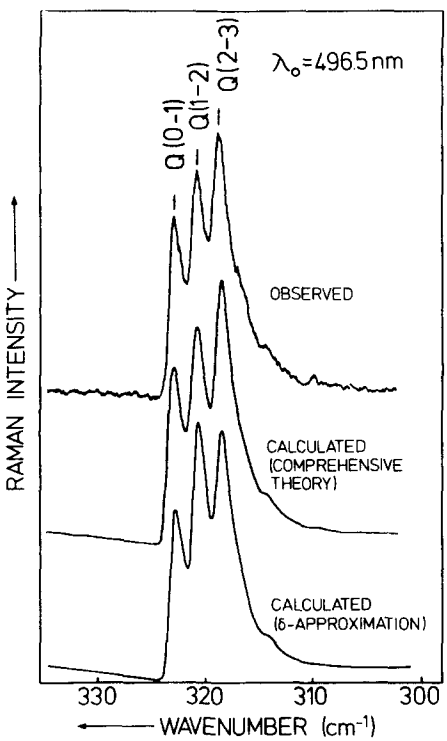

FIG. 12. Captions as in Fig. 9 except for $\lambda_0 = 496.5$ nm.

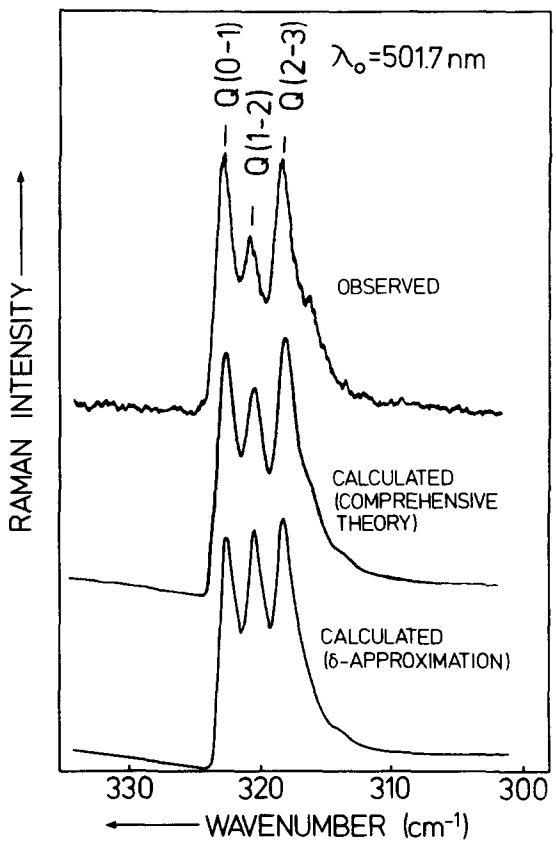

FIG. 13. Captions as in Fig. 9 except for $\lambda_0 = 501.7$ nm.

Quantitative calculations by means of the δ approximation are shown in Fig. 14, where we display the band profiles calculated for the two excitation wavelengths and separated into the contributions from the two electronic states. The spectra labeled by $^1\Pi$ and B corre-

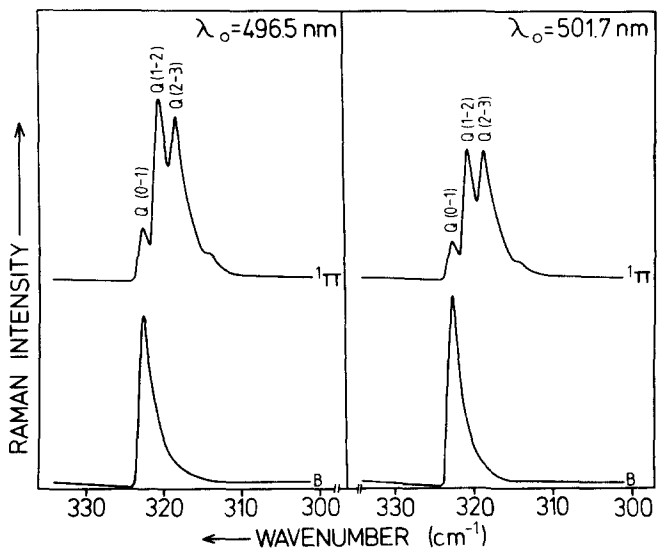

FIG. 14. Calculated continuum resonance Raman spectra of the fundamental of $^{79}Br_2$ (δ approximation) for $\lambda_0 = 496.5$ nm (left field) and $\lambda_0 = 501.7$ nm (right field) excitation. Shown are the contributions from the continuum of the $^1\Pi$ state alone (upper spectra) and from the continuum plus the discrete levels of B state (lower spectra).

spond to the first and second term of Eq. (2) of Ref. 37, respectively, and thus reflect the neat contribution from the $^1\Pi$ and B states alone. Note that the third term of Eq. (2) of Ref. 37, which describes the interference between both states,[33] is not taken into account for the calculation of the spectra displayed in Fig. 14. Since in $^{79}Br_2$ the slope of the dissociative B state is slightly steeper than the one for the repulsive $^1\Pi$ state for equal energy (compare the slopes of the two potential curves to each other, for example, at the energy of the intermediate state for each of the diagrams shown in Figs. 3–6), the error made through the δ approximation for the $1 \leftarrow 0$ transition may be smaller than the one for transitions which originate from contributions mainly through the $^1\Pi$ state. Furthermore, one can compare the two transitions which are generated through resonance mainly with the repulsive state, to each other. Since the intermediate state of the $3 \leftarrow 2$ vibrational Raman transition has higher energy than the $2 \leftarrow 1$ transition and hence the slope of the $^1\Pi$ potential curve at the intermediate state energy is steeper for the $3 \leftarrow 2$ than for the $2 \leftarrow 1$ transition, it is expected that the error made by the δ approximation is smaller for the $3 \leftarrow 2$ transition. Comparing the slopes of the potential curves at the various intermediate Raman levels with the deviations from exact and approximative δ calculations, we can derive a rough estimation: as long as the slopes $|dV/dR|$ (V = potential function; R = internuclear separation) are higher than about 30 000 $cm^{-1}/Å$, the error made by employing the δ approximation (as compared to the comprehensive theory) can be neglected for the scattering system studied. As far as we know, this is the first time a check of the δ approximation against the complete calculation for vibrational intensities in RRS has been performed.

The δ-approximation method and the diagrams as displayed in Figs. 3–6 can serve also to give a qualitative explanation of the changes in intensity of the observed vibrational transitions. Let us focus first on the $1 \leftarrow 0$ and $2 \leftarrow 1$ transitions when excited with $\lambda_0 = 457.9$ nm (Figs. 3–4 and Fig. 9). Qualitatively we may obtain a value for the product of the two VOF's and hence for the vibrational Raman scattering amplitude by multiplying the vertical bars for the absorption and the re-emission process for each of the two states (B and $^1\Pi$). If we do so, the Raman amplitude for the $2 \leftarrow 1$ transition would be smaller than the one for the $1 \leftarrow 0$ transition because the bars for the re-emission for the $2 \leftarrow 1$ transition are smaller than the correspondent bars for the $1 \leftarrow 0$ transition, in contrast to the observation made in the experiment. Figure 9 shows that the intensity (square of the Raman scattering amplitude) of transition $2 \leftarrow 1$ is about two times greater than the intensity of the $1 \leftarrow 0$ transition. However, Fig. 3 shows that the sign of the Raman scattering amplitude originating from the B state is opposite to the sign of the Raman amplitude originating from the Π state for the $1 \leftarrow 0$ transition, because the amplitude of the wave function $v = 1$ at the position of the classical turning point for the B state is negative and the other three amplitudes are all positive (see Fig. 3). For the $2 \leftarrow 1$ transition, however, the signs of the Raman amplitudes for both states are positive (see Fig. 4), because for the B state the amplitude of the wave function is negative for the absorption as well as re-emission process and for the $^1\Pi$ state both amplitudes of the wave functions are positive. If we now take into consideration, that opposite signs of Raman amplitudes lead to destructive interference, whereas equal signs to constructive interference (third term in Eq. 2 of Ref. 37), we understand why the $1 \leftarrow 0$ transition shows smaller intensity than the $2 \leftarrow 1$ transition for this excitation. Such interference effects have been already shown by us earlier by applying the comprehensive theory.[33,37]

Another feature in the RR spectra of bromine vapor can be nicely explained by means of the simple method described above. If we compare Fig. 11 with Fig. 9 we recognize a strong $3 \leftarrow 2$ transition for 488 nm excitation (Fig. 11), while this band is completely missing when the wavelength 457.9 nm (Fig. 9) is used for excitation. A view on to the diagrams displayed in Figs. 6 and 5 immediately explains this behavior. In Fig. 5 we recognize that by accident the wave function for the initial vibrational state ($v = 2$) has zero amplitude at the position of the classical turning point for both the B and $^1\Pi$ state. As a consequence, both states do not contribute at all to the Raman scattering amplitude resulting in zero intensity for this transition and 457.9 nm excitation. However, the amplitudes of the wave functions of initial ($v = 2$) and final ($v = 3$) vibrational state have an appreciable value for 488 nm excitation (see Fig. 11) which leads to observable Raman intensity in this case (see Fig. 9). Similarly, the intensities of all other bands displayed in Figs. 9–13 can be explained qualitatively in this way.

IV. CONCLUSION

We have shown how the δ approximation or reflection method can be applied to the calculation of continuum resonance Raman spectra of diatomic molecules. Satisfactory agreement between theoretical and experimentally observed intensity distributions was found. It was shown that the δ approximation works well for steep excited state potential curves. The main advantage so far is not only the reduction in computational time (about 50% compared to the comprehensive theory), but also the fact that calculations of RR intensities can be performed without knowledge of the excited state continuum wave functions. Therefore, first principle calculations of continuum resonance Raman spectra for molecules with more than two atoms may become possible in the future.

ACKNOWLEDGMENT

We wish to thank the Leibniz Rechenzentrum, Munich, for grants of computer time.

[1] E. U. Condon, Phys. Rev. **32**, 858 (1928).
[2] J. G. Winans and E. C. G. Stueckelberg, Proc. Natl. Acad. Sci. U.S.A. **14**, 867 (1928).
[3] E. C. G. Stueckelberg, Phys. Rev. **42**, 518 (1932).
[4] W. H. Miller, J. Chem. Phys. **48**, 464 (1968).
[5] F. H. Mies, J. Chem. Phys. **48**, 482 (1968).
[6] R. S. Mulliken, J. Chem. Phys. **55**, 309 (1971).

[7]I. Riess, J. Chem. Phys. **56**, 1613 (1972).
[8]C. F. Goodeve and A. W. C. Taylor, Proc. R. Soc. London Ser. A **152**, 221 (1935).
[9]A. S. Coolidge, H. M. James, and R. D. Present, J. Chem. Phys. **4**, 193 (1936).
[10]N. S. Bayliss, Proc. Phys. Soc. London Sect. A **158**, 551 (1937).
[11]H. M. James and A. S. Coolidge, Phys. Rev. **55**, 184 (1939).
[12]N. S. Bayliss and A. L. G. Rees, J. Chem. Phys. **8**, 377 (1940).
[13]G. Herzberg, *Spectra of Diatomic Molecules* (Van Nostrand, Princeton, 1950), p. 393.
[14]G. H. Dunn and L. J. Kieffer, Phys. Rev. **132**, 2109 (1963).
[15]L. J. Kieffer and G. H. Dunn, Phys. Rev. **158**, 62 (1967).
[16]G. H. Dunn, Phys. Rev. **172**, 1 (1968).
[17]E. A. Gislason, J. Chem. Phys. **58**, 3702 (1973).
[18]R. J. Leroy, R. G. MacDonald, and G. Burns, J. Chem. Phys. **65**, 1485 (1976).
[19]W. Holzer, W. F. Murphy, and H. J. Bernstein, J. Chem. Phys. **52**, 399 (1970).
[20]For a recent review see D. L. Rousseau, J. M. Friedman, and P. F. Williams, in *Raman Spectroscopy of Gases and Liquids*, *Topics in Current Physics*, edited by A. Weber (Springer, Berlin, 1979), Vol. 11, pp. 203–252.
[21]M. Mingardi and W. Siebrand, Chem. Phys. Lett. **23**, 1 (1973).
[22]M. Mingardi and W. Siebrand, J. Chem. Phys. **62**, 1074 (1975).
[23]M. Jacon and D. van Labeke, Mol. Phys. **29**, 1241 (1975).
[24]P. R. Fenstermacher and R. H. Callender, Opt. Commun. **10**, 181 (1974).
[25]R. J. LeRoy, J. Chem. Phys. **52**, 2683 (1970).
[26]W. Kiefer and H. W. Schrötter, J. Chem. Phys. **53**, 1612 (1970).
[27]W. Kiefer and H. J. Bernstein, J. Chem. Phys. **57**, 3017 (1972).
[28]W. Kiefer and H. J. Bernstein, J. Mol. Spectrosc. **43**, 366 (1972).
[29]W. Kiefer and H. J. Bernstein, J. Raman Spectrosc. **1**, 417 (1973).
[30]W. Kiefer, Appl. Spectrosc. **28**, 215 (1974).
[31]P. Baierl and W. Kiefer, J. Chem. Phys. **62**, 306 (1975).
[32]P. Baierl and W. Kiefer, J. Raman Spectrosc. **3**, 353 (1975).
[33]P. Baierl, W. Kiefer, P. F. Williams, and D. L. Rousseau, Chem. Phys. Lett. **50**, 57 (1977).
[34]W. Kiefer and P. Baierl, Indian J. Pure Appl. Phys. **16**, 171 (1978).
[35]W. Kiefer and P. Baierl, in *Laserspektroskopie*, edited by F. Aussenegg (Springer, Wien, 1979), p. 43.
[36]P. Baierl and W. Kiefer, J. Raman Spectrosc. **10**, 197 (1981).
[37]P. Baierl and W. Kiefer, J. Raman Spectrosc. **11**, 393 (1981).
[38]F. H. Mies and P. S. Julienne, IEEE J. Quantum Electron. **QE-15**, 272 (1979).
[39]D. L. Rousseau and P. F. Williams, J. Chem. Phys. **64**, 3519 (1976).
[40]S. Y. Lee and E. J. Heller, J. Chem. Phys. **71**, 4777 (1979).